Cuffless Blood Pressure Estimation

PDSB 2021 – Group B1
Diogo Antunes, no. 86979,
Diogo Batista, no. 86767,
Pedro Osório, no. 89777

1. ABSTRACT

The goal of this project was to derive blood pressure measures using a combination of different features extracted from PPG and ECG signals. The motivation behind it is the existing need for continuous and cuffless blood pressure measurement techniques, allowing the obtention of more valuable data about the patient's health status in a more comfortable manner. With that in mind, we developed a set of *MATLAB* scripts and functions that enabled us preprocess PPG and ECG signals and then extract from them 21 blood pressure related physiological parameters that worked as predictors of a set of final multivariate linear regression models for blood pressure estimation. We used a dataset composed of multiple hours of signals from two patients. A PCA was performed, finding that there was no clear predominance of variance explained by a specific group of features and that the main source of variance within our dataset was the subject from where they were each sample was extracted. Dimensionality reduction was achieved through a stepwise linear regression model, revealing 3 features to be the most relevant for the prediction. The cross-validation of our models revealed results that were comparable to the ones from the literature, however affected by the limitations stemming from our dataset not being representative.

2. PROBLEM AND MOTIVATION

Hypertension, also known as the silent killer, is one of the main risk factors for prevalence of cardiovascular diseases. According to the World Health Organization hypertension prevalence is of 24 percent for men and 20.5 for women [1], while the European Heart Journal reports that 4.1 million people die annually due to cardiovascular disease, making it the number one cause of death in the region [2].

In order to diagnose and prevent hypertension and cardiovascular disease accurately, Blood pressure (BP) measurement must be regularly done. BP can be interpreted as a physiological variable comprising of several pulse waves which vary both in amplitude and frequency. It is highly dynamic with significant continuous changes occurring over different time periods, which can span from minute to minute, hour to hour, or during the different activities throughout the day. Oscillations are also visible over longer time periods spanning days or even months. Several factors lead to these fluctuations, which are a result of the homeostatic response of the circulatory system, and they can be due to sleep, physical activity or even food intake. The most clinically relevant fluctuations are those caused by pathologies responsible for disfunction of factors that modulate cardiac flow. There is evidence that identifying these changes can be of major clinical importance, mainly in prognostic situations, since augmented BP oscillations are correlated to higher risk of cardiovascular events, organ damage and mortality [3]. A continuous twenty-four-hour BP measurement procedure can then be an important tool in monitoring blood pressure throughout the day and provide highly relevant data.

3. BACKGROUND AND RELATED WORK

Cuff based inflation methods are still the standard practice for measuring blood pressure, as well as auscultatory methods based on Korotkoff sounds. Although useful in clinical environments these carry several limitations, namely their inaccuracy, impossibility to obtain continuous measurements of patient's BP in order to capture fluctuations over time, both during the day and during sleep, and also the discomfort and pain they may cause. The difficulty in measuring of BP over the night and during sleep has led to there still be uncertainty regarding clinical problems such as assessing the relationship between hypertension and obstructive sleep apnoea or understanding the high frequency of stroke and heart attacks during the sleep.

There is then a demand for the development of methods that allow continuous cuffless BP monitoring.

Several approaches are available, although not widely applied due to difficulties in their implementation. One that has been available for a longer time is the measurement of intraarterial beat-by-beat BP recordings. This, however, is an invasive approach which for obvious reasons debilitates its applicability in continuous monitoring. A non-invasive approach is the volume-clamp method which was implemented in the commercially available Portapres and Finapres systems. These are widely used in research, however in more daily and common uses it is not the most convenient due to its high cost and difficulties in calibration.

Mobile based approaches relying on apps have also surfaced. These have yet to be studied enough, with no validation studies having been conducting for most of the available smartphone applications focused on BP measurement, and several having shown lower accuracy than cuff inflation methods [4].

Finally, there are the approaches based on pulse wave propagation which is used to derive models used to compute BP, based either on pulse transit time (PTT) measurement in which a stretch-strain relationship is derived or other pulse wave analysis methods. These make use of the electrocardiogram (ECG), photoplethysmogram (PPG) and ballistocardiogram (BCG) which can be obtained in a nonobtrusive manner. Wave propagation through the tissues is highly dependent on the relationship between transmural pressure and the mechanical properties of the arterial vessel wall. This a critical property of the human circulatory system, which is pressurized, where the pressure inside the vessel is majorly influenced by the wall's stiffness. The bulk modulus of a material is determinant in wave propagation through it, and so, the speed of disturbances caused by cardiac effort travelling through the arterial vessel is related to the stiffness of the wall.

Hence, the velocity of a traveling pulsed wave can be interpreted as a measure of arterial blood pressure. This is the base principle that allows pulse wave velocity (PWV) measurement to lead to arterial pressure computation. Pulse transit time (PTT) variation corresponds to changes of PWV in a fixed distance, which is an indicator of variation of BP. PTT can be seen as more robust measure of BP than other procedures, like oscillometric or auscultatory methods [5].

Several wave property features can be extracted and different approaches can be taken, namely heuristic modelling with regression[6], [7] , which normally make use of the Moens-Korteweg formula, or predictive modelling resorting to machine learning algorithms [8]–[10] . The methods can also be distinguished on the type of features used. There are the physiological based, which are derived from physiological parameters from vital signals. These result in small sized vectors which require an acceptable training computation. However, signal morphology can vary between samples, with some displaying nonideal shapes, making it more arduous to extract information. On the other hand, the feature selection can be automated by having a whole-based representation of the signals and making use of non-linear learning algorithms. While this approach is more robust to the variation in shape of the signals, the resulting vectors are larger which requires more samples for the model training and also results in longer computation.

4. APPROACH AND UNIQUENESS

4.1 Material

We were provided with a dataset of 6 subjects from the MIMIC-II and MIMIC-III databases [11] with several real sets biological data. From this array of subjects, only three simultaneously presented photoplethysmography (PPG), electrocardiography (ECG) and arterial blood pressure (ABP) data and, adding to that, only two of those presented interpretable PPG data as the third one was saturated for most of its length. We therefore considered the data from only two subjects, coincidentally from the MIMIC-II database.

The target values of systolic blood pressure (SBP) and diastolic blood pressure (DBP) were estimated from the ABP curves, and the features were extracted from both ECG and PPG waveforms, however it should be noted that since the data is from intensive care unit (ICU) patients the parameters extracted is prone to abnormal variations related to administered drugs and underlying pathologies.

We developed a set of functions and scripts in MATLAB which enabled us to perform all the below mentioned processing, feature extraction, principal component analysis (PCA) and estimation model. All the ".m" files and data are delivered alongside this paper.

4.2 Methods

4.2.1 Data preprocessing

At a first stage, NaNs are removed across all signals, preserving their alignment in each subject. The PPG data is normalized as it was in a different range of values in each subject. The ECG and ABP data were not normalized as we only intended to extract time domain characteristics from the former and we did not want to lose the original units from the latter, as we wanted the final model to predict the SBP and the DBP in conventional ABP units (mmHg).

Next, a wavelet denoising in the low frequencies is performed on the ECG and PPG data to remove breathing artifacts ("wandering baseline") in the signals, by discarding the last four detail wavelet transform coefficients: d_7, d_8, d_9, and d_{10}, and the approximation coefficient a_{10}. For this purpose, we employed the Daubechies 8 mother wavelet and obtained 10 decomposition levels, similarly to [9]. We opted for this denoising method mainly due a better phase response, better computational efficiency and better adaptivity to these biological signals [9].

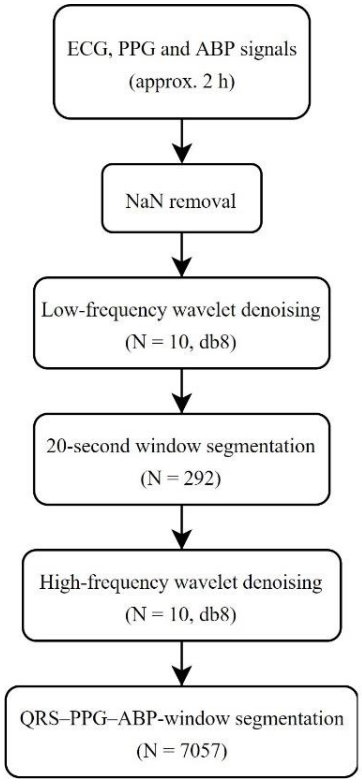

Figure 1: Signal preprocessing pipeline.

The abovementioned processing will cause the loss of the inherent offset of the PPG data; therefore, we added the mean of the original signal to the filtered one to account for that effect. This way we can still maintain some of the physiological meaning of the PIR feature which, as we will address later, depends on the maximum and minimum intensity of the PPG signal within a cardiac cycle.

After the NaN removal and low-frequency denoising, the three signals are cropped into 20-second segments, and all the segments whose minimum and/or maximum values are below or above specific thresholds, respectively, are discarded. The upper and lower thresholds are computed as

$$threshold_k = \mu_k \pm a\,\sigma_k, \qquad a > 0, \tag{1}$$

where μ_k and σ_k are the signal k's mean and standard deviation, respectively, and a is a positive scalar that was adjusted to each signal subject. Whenever a signal's segment is rejected, the other two signals' segments in the same time interval are also rejected, to preserve the alignment.

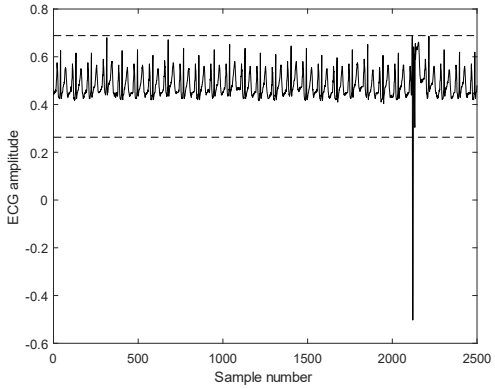

Figure 2: A rejected 20-second ECG window with its minimum amplitude (an artifact) below the lower threshold.

The following step was to perform a high frequency wavelet denoising of every 20-second window obtained from the previous step, employing the Daubechies 8 mother wavelet, 10 decomposition levels and the soft *Rigrsure* thresholding strategy with a threshold rescaling based on a noise estimated from the first-level coefficients. MATLAB's *Wavelet Toolbox*'s function *wden.m* was used for this purpose.

The final processing step was to segment each set of homologous 20-second windows of denoised ECG, PPG and ABP signal into smaller segments containing fewer cardiac cycles which will serve as input of the feature extraction functions. With that in mind, we proceeded to perform a *sym4* mother wavelet, 4-level wavelet decomposition of the ECG waveforms in each 20-second windows and, by reconstructing only with the 2nd and 3rd detail coefficients, we get an ECG signal where the R peaks are significantly more noticeable and more easily detectable. This step is quite relevant as it helps us detect the time location of the R peaks in each window more accurately, thereby removing the possibility of detecting abnormally large P or T waves. The peak detection was made with the MATLAB's *Signal Processing Toolbox*'s function *findpeaks.m*.

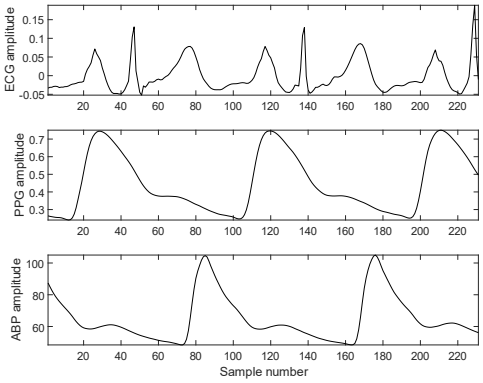

Figure 3: An example of an ECG–PPG–ABP window that will work as an input sample of our feature extraction pipeline.

Once the locations of each R peaks are detected we finally segmented each set of ECG, PPG and ABP signals in several sets of homologous intervals "centered" around each detected R peak. Each interval starts at half the distance between the current R peak and the previous R peak, and extends up until the second R peak at the right of the current R peak (see **Figure 3**). This interval will then include approximately three PPG pulses, the previous, the current and the initial part of the next one as this signal is acquired distally (probably at the finger) of the heart thus having a time shift in relation to the ECG. The ABP signal, since it is also measured distally follows the same pattern but with a shorter time shift, suggesting it was measured closer to the heart than the PPG. The ABP window includes part of the previous pulse, the current one and part of the next one.

4.2.2 Feature Extraction

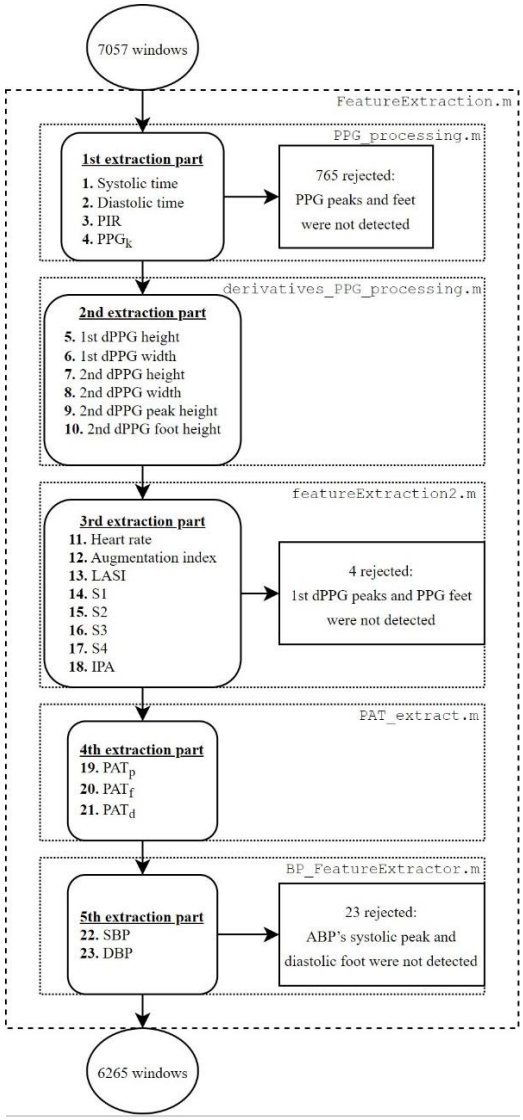

Figure 4: Feature extraction pipeline, with the identification of the functions in use at each step. Windows can be interpreted as samples for the estimation model.

The extraction of features in the ECG–PPG window related to the blood pressure is parameter-based as opposed to whole-based, briefly mentioned in Section 3. A total of 21 features are extracted from the shape of the PPG signal and its derivatives as well as from the time shift between the ECG and PPG waves.

Information from the PPG derivatives is considered in our model as previous studies have shown that it is useful for the evaluation

of the degree of arteriosclerosis [12]which, in turn, is well correlated with the mean blood pressure inside a blood vessel [13].

It has also been shown that the blood pressure can be inferred from the pulse transit time (PTT) [14] [15] [16], which is the length of the time interval from the mechanical movement of the heart and the arrival of the pulse at the distal point [9]. We can then use the pulse arrival time (PAT) as a measure of PTT in our model, as they represent the same amount only differing on the fact that the former also considers the duration of the electrical activation of the heart just before its movement, which is very short. This is usually done as the PAT is more convenient to measure, representing the length of the time interval between the ECG's R peak and the respective PPG's pulse measured at a distal point. Three different measures of PAT were considered in our model.

Another feature which is relevant to mention is the PPG's pulse intensity ratio (PIR), which has also been showed to be inversely proportional to the DBP.

The features are represented in **Figure 5** and the full list of them goes as follows:

- *Systolic time* (ST, f_1): Ascending time from PPG foot to its systolic Peak.
- *Diastolic time* (DT, f_2): Descending time from PPG systolic peak to the next PPG wave diastolic foot.
- *Pulse intensity ratio* (PIR, f_3)*:* Ratio of the intensity of the PPG's systolic peak and diastolic foot.
- *Heart rate* (HR, f_4): Inverse of the duration between consecutive ECG R peaks.
- *Pulse arrival time (*PAT*):* Time span between the ECG's R peak and the PPG's systolic peak (PAT_p, f_5), diastolic foot (PAT_f, f_6) and maximum slope point (1st derivative peak value) (PAT_d, f_7).
- *Augmentation index* (AI, f_8): Measure of the pressure waves reflection on arteries and it is computed through the ration of the PPG pulse peak intensity and the intensity of the inflection point closer to the diastolic peak.
- *Large artery stiffness index* (LASI, f_9): Inverse of the time span from the PPG's systolic peak to the inflexion point closest to the diastolic peak.
- *S1, S2, S3* and *S4*: Areas under the PPG pulse curve from the diastolic foot to the point of max slope (S1, f_{10}), from the latter to the systolic peak (S2, f_{11}), from the latter to the inflexion point closest to the diastolic peak (S3, f_{12}), from the latter to next pulse's diastolic foot (S4, f_{13}).
- *Inflection point area ratio* (IPA, f_{14}): Ratio of S4 over the sum of S1, S2 and S3, $\mathrm{IPA} = \mathrm{S4}/(\mathrm{S1} + \mathrm{S2} + \mathrm{S3})$. It is a measure of total peripheral resistance, a factor known to influence blood pressure, as it represents the resistance the blood encounters when flowing through the vessels [17].
- *PPG characteristic value* (PPG_k, f_{15}):

$$\mathrm{PPG_k} = \frac{p_m - p_d}{p_s - p_d} \quad (2)$$

  Where p_m is the area under the curve (S1 + S2 + S3 + S4) divided by the pulse duration, p_d is PPG's minimum intensity and p_s its maximum intensity.
- *PPG's 1st derivative characteristics:* Maximum intensity (dppgH, f_{16}) and time span between maximum and minimum values (dppgW, f_{17}).
- *PPG's 2nd derivative characteristics:* Maximum intensity (ddppgPH, f_{18}), absolute value of minimum intensity (dppgFH, f_{19}), sum of the two latter features (ddppgH, f_{20}), time span between maximum and minimum values (ddppgW, f_{21}).

The features that required peak detection were extracted by means of the *findpeaks.m* MATLAB function with the adequate settings of *minimum peak height* and *minimum distance between peaks*. The former setting was defined like in Equation 1 and the latter was defined according to the normal range of heart rate values, discarding peaks that were too close to the next PPG pulse's peaks.

The features related to the areas under the PPG curve were computed through the *trapz.m* MATLAB function, which relies on the *trapezoidal rule approximation method* to numerically integrate the input curve between user specified points.

As it is depicted in **Figure 4**, the previously generated windows of signal are fed as input of the *FeatureExtraction.m* function, and the feature extraction is done at various steps relying on several other functions implemented by us. At each stage, the widows go through quality control, being discarded if they do not contain interpretable signal, that is if the well documented features of each signal are not present. This is an important step as, even though the noise and large amplitude artifacts have been removed during the preprocessing, there can still be low amplitude artifacts that contaminate our samples.

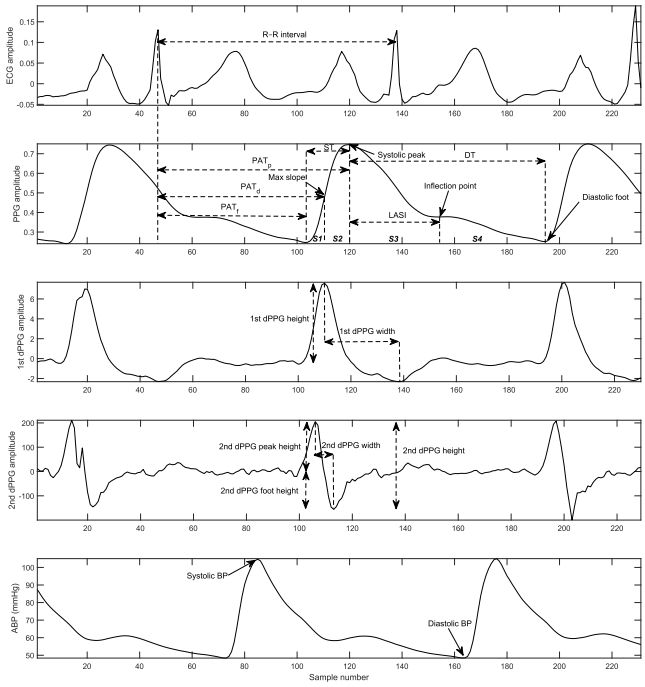

Figure 5: Extraction of the signal features as well as the target values of SBP and DBP.

4.2.3 Dimensionality Reduction

A relevant step in our project was performing a PCA as an attempt to understand which features were responsible for the most variance within our dataset and possibly discard the ones that account for less variance.

Reducing the number of predictors is especially useful to increase the computational efficiency of our model's training process, as larger predictor vectors lead to increased computation times. The computational efficiency of the training process becomes even

more relevant when performing cross-validation tests, like *leave-one-out*, as the training procedure is made repeatedly.

Another method that could have been used for dimensionality reduction is assessing the level of correlation among our set of features based on the way they are extracted and then, if that is the case, we can remove the ones that hold redundant information.

An additional alternative, which we end up using, was to use a *stepwise linear regression*, in which, as we will address in the next section, the features to be included in the model are selected according to their statistical significance in the regression.

4.2.4 Stepwise Multivariate Linear Regression

A stepwise regression is performed with the signals' features to create linear models capable of predicting SBP and DBP values,

$$SBP = \alpha_0 + \alpha_1 f_1 + \alpha_2 f_2 + \cdots + \alpha_n f_n \quad (2)$$

and

$$DBP = \beta_0 + \beta_1 f_1 + \beta_2 f_2 + \cdots + \beta_n f_n, \quad (3)$$

where α_i and β_i are the estimated coefficients, and f_i is the value of feature i. With stepwise regression, a series of steps are done where, starting from an empty set of predictors, a feature is added to or removed from the model based on the likeliness of it having a null coefficient. This likeliness is measured by computing and comparing the *p*-value of an *F*-statistic with a predefined threshold (default is 0.05). The method stops when no removal or addition of features improves the model. The method of least squares is used to compute the coefficients.

Three datasets were considered as training sets for the regression: (i) both subjects' signal features, (ii) Subject 1's only, and (iii) Subject 2's only. Then, the respective models were evaluated choosing all the windows from (i) Subject 1 and 2, (ii) Subject 1, and (iii) Subject 2 as testing sets, with leave-one-out cross-validation. The two models with training sets containing only one of the subjects' information are also evaluated with the other subject's data, to confirm the presence of a bias in the models, that is, the models show worse results when estimating SBP and DBP values of the subject excluded from the training set. The mean absolute error (MAE), standard deviation (STD), and root-mean-squared error (RMSE) were determined for each case.

5. RESULTS

5.1 Dimensionality Reduction

5.1.1 Principal Component Analysis

When considering the whole spectrum of samples, we get that the component that explains the most variance, only explains about half of it (**Figure 6**). Adding to that, once we analyze the contribution of each feature to this component, we see that every feature contributes about the same amount to it (**Figure 7**), thereby being hard to justify any feature selection and dimensionality reduction based on these results. In fact, in terms of estimation model accuracy, it is only useful to reduce the number of features based on a PCA when there is a clear dominance of some features over others regarding explained variance, which is not the case.

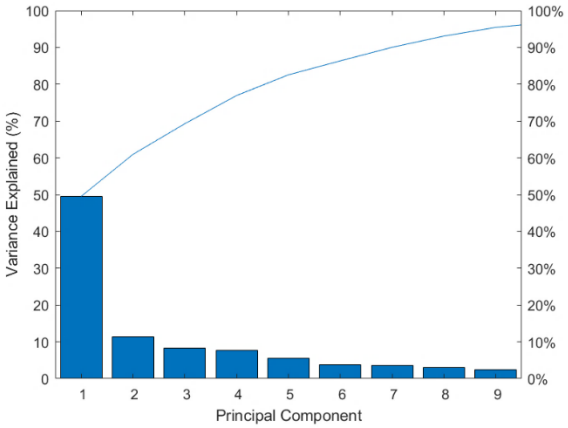

Figure 6: Scree-plot depicting the percentage of total variance explained by each principal component.

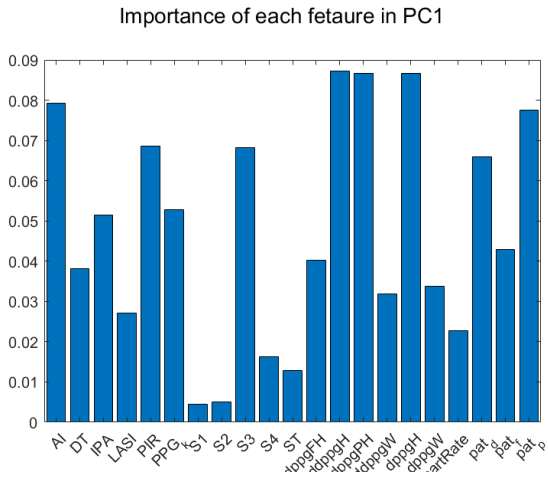

Figure 7: Relative weightings of each feature in the first principal component.

However, having the projection of our dataset on the plane defined by the two first principal components (most variance-explaining plane), we can clearly see that our samples cluster into two different groups. These two groups clearly correlate to the two different sources of data used in this project, Subject 1 and Subject 2 (**Figure 8**).

What we take from this is that the main source of variance within this dataset is the origin of the samples. In fact, this would be expected as the MIMIC-II database provides data for different subjects, with different health statuses, different physiological characteristics and, adding to that, acquired in different environments and with different instrumentation.

Had we used a larger dataset with acquisitions from a larger number of patients we could minimize the effect of this source variance and the main source of variance would shift to the actual extracted features.

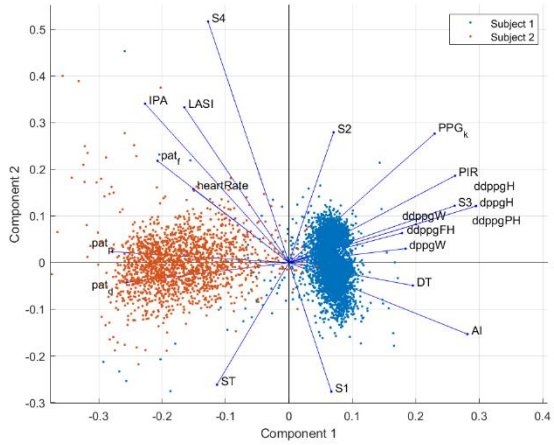

Figure 8: Projection of the dataset onto the plane defined by the first two PC and projections of each feature on the same plane.

If we analyze the subsets related to each subject separately, we can see that in both cases the first principal components account for even less of the total variance in the dataset, meaning the variance is even more homogeneously explained through the features than when considering the whole dataset (**Figure 9**).

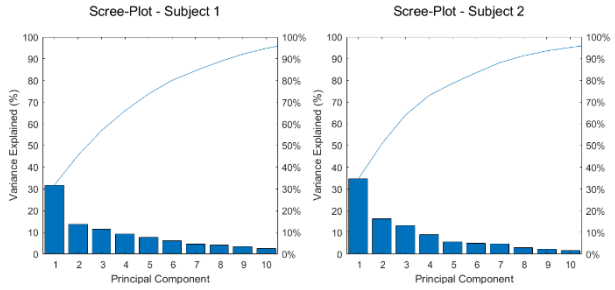

Figure 9: Scree-plot depicting the percentage of total variance explained by each principal component in each subject subset.

Analyzing the features weights on the first principal component of each subset (**Figure 10**) we can understand that the variance explained by each feature is similar between subjects. Features ddppgH, ddppgPH and dppgH seems to explain a similar relative amount of variance in both subsets whereas S4 explains a large amount of the variance in Subject 1 but a unsignificant amount in Subject 2. What is also relevant to note is that there are features like DT, PAT_d and PAT_p that in both subsets do not explain much variance but, when considering the whole dataset, they start to explain more. These are the features whose variance is most associated to the variance resulting from the differences between the patients.

As a final comment, from **Figure 8** we can see that the Subject 2 subset appears to be more varied than Subject 1's, which was expected considering that Subject 2's PPG signal's amplitude varied much more throughout the samples (**Figure 11**).

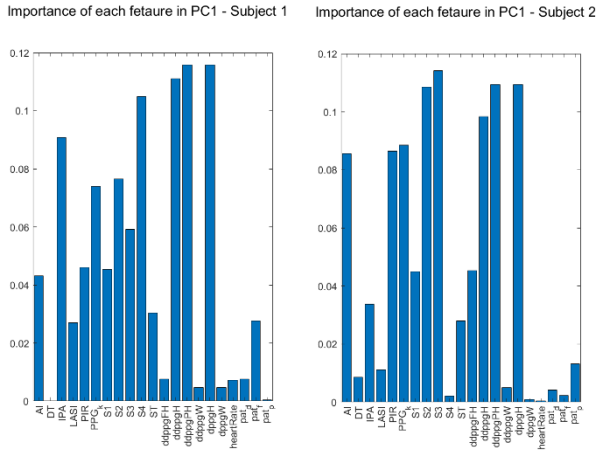

Figure 10: Relative weightings of each feature in the first principal component of each subset.

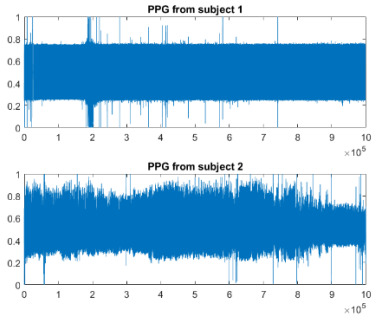

Figure 11: Low frequency denoised PPG signal from Subject 1 (top) and Subject 2 (bottom).

5.1.2 Stepwise Multivariate Linear Regression

In **Table 1** we can see the features that were selected or removed by the stepwise linear regression algorithm depending on the training used and on the type of target value (SBP or DBP).

As a first comment, we see that a lot more features are considered not statistically significant for the regression based on Subject 2's subset. This might be related to the fact that this patient, as we have mentioned before, provided data with a lot more variance in contrast to Subject 1's.

We find that f_{18}, ddppgPH, is removed with every training set meaning that there is a significant chance of its model's coefficient being zero thereby not being as much correlated with both SBP and DBP as the other features. The PAT_f, parameter, f_6, is removed from the predictor vector in every training set, only being considered when estimating DBP with Subject 1's subset. This also tell us that this feature is not so well correlated to blood pressure as the others.

Based on our samples, the features that we expect to be the most correlated to the blood pressure values are the ones that were never discarded when applying the model to each training set. The features in that situation are f_8, f_{14} and f_{15} which refer AI, IPA and PPG_k, respectively.

However, it is important to note that the quality of the fit, and hence the array of features considered statistically significant for the regression, depend on what the set of features introduced for the initial model in the *stepwisefit.m* function algorithm was. In other words, the algorithm is only able to find a locally optimal fit and not the globally optimal, meaning that we have no guarantee that if

we had used a different combination of features for the initial model (instead of an empty vector with only a constant) we could have obtained better fit [18].

Another factor that we should also have in mind, is that our remarks are only based on a sample size of two subjects, therefore being extremely limited in terms of applicability to samples of other people. All in all, the features we here observe to be the most relevant could have been completely different had the dimension of the training sets been larger and contained data from other patients, with different physiological characteristics and health statuses.

Table 1: Features discarded (X) when performing the stepwise linear regression with the various subsets.

Training set		f_1	f_2	f_3	f_4	f_5	f_6	f_7	f_8	f_9	f_{10}	f_{11}	f_{12}	f_{13}	f_{14}	f_{15}	f_{16}	f_{17}	f_{18}	f_{19}	f_{20}	f_{21}
Subject 1 and 2	SBP			X			X										X	X	X			
	DBP						X											X	X		X	
Subject 1 only	SBP	X					X												X	X		X
	DBP	X									X						X		X			X
Subject 2 only	SBP	X	X	X	X		X	X		X			X	X				X	X	X	X	X
	DBP	X			X	X	X	X		X	X	X	X				X	X	X	X		X

Table 2: Root-mean-squared errors of the linear models for each training subset with respective SBP and DBP variances

	Systolic blood pressure		Diastolic blood pressure (mmHg)	
Training set	RMSE (mmHg)	Variance ($mmHg^2$)	RMSE (mmHg)	Variance ($mmHg^2$)
Subject 1 and 2	7.42	77.9	3.83	51.2
Subject 1 only	4.38	38.5	1.53	6.6
Subject 2 only	10.59	171.1	5.89	51.5

Table 3: MAEs, STDs, and RMSEs of the cross-validation of the linear models

	Systolic blood pressure (mmHg)			Diastolic blood pressure (mmHg)		
Training set	MAE ([9])	STD ([9])	RMSE	MAE ([1])	STD ([1])	RMSE
Subject 1 and 2	4.65 (14.71)	7.52 (10.79)	7.52	2.10 (6.74)	3.92 (6.11)	3.92
Subject 1 only	3.30	3.08	4.52	1.10	1.12	1.56
Subject 2 only	6.56	8.469	10.71	3.47	4.79	5.91

Table 4: MAE, STD, and RMSE of the linear models with alternating training and testing sets

		Systolic blood pressure (mmHg)			Diastolic blood pressure (mmHg)		
Training set	Testing set	MAE	STD	RMSE	MAE	STD	RMSE
Subject 1	Subject 2	13.23	10.78	17.06	9.22	6.33	11.18
Subject 2	Subject 1	36.79	7.00	37.45	22.40	3.62	22.69

5.2 Estimation Models

5.2.1 Stepwise Multivariate Linear Regression

The RMSE values displayed in **Table 2** show how well the linear regressions fit the datasets. Subject 1's models have the lowest RMSEs, 4.38 mmHg (SBP) and 1.53 mmHg (DBP), thus showing a better linear correlation between features. Subject 2's models have the highest RMSEs of the three datasets, 10.59 mmHg (SBP) and 5.89 mmHg (DBP), displaying a worse linear correlation between features compared to Subject 1's models. Therefore, the models containing both subjects' information have RMSE values in-between, 7.42 mmHg (SBP) and 3.83 mmHg (DBP).

What is also relevant to note, is that we can find smaller RMSE and STD for the models estimating DBP as opposed to SBP. We can expect this to be due to the fact that DBP is prone to less variance than SBP (**Table 2** and according to what is found in [9]). A similar effect is observable when comparing the RMSE and STD of the fits when considering Subject 1's subset with Subject 2's, as the latter are larger due to lesser quality and more varied signal (**Figure 11**).

The models' ability to generalize to an independent set was analyzed through leave-one-out cross-validation (**Table 3**). The models obtained from the two subjects have the drawback of being limited by the number of subjects in the dataset, thus being unlikely to be to be accurate at estimating another subject's SBP and DBP, other than Subject 1 and 2. Comparing the models with both subjects' information with [9], whose parameter-based linear regressions' MAE (STD) values for the SBP and DBP are 14.71 mmHg (10.79 mmHg) and 6.74 mmHg (6.11 mmHg), respectively, our models' MAE and STD values are lower; however, their models' dataset contains approximately one thousand subjects, many of whom likely have features with worse linear correlations between them (akin to Subject 2) that increase the models' MAE and STD values.

The models' containing only Subject 1's information have lower MAE, STD, and RMSE values compared to Subject 2, which further shows the former models are more capable of predicting Subject 1's SBP and DBP than the latter with respect to Subject 2. The poorer quality and higher fluctuation of Subject 2's signals are likely to affect the models' prediction accuracy.

The models' containing only one of the subjects' information are also tested with the other subject's information (**Table 4**) to conclude that the MAE, STD, and RMSE are greater, which is observed when comparing with **Table 2**'s and **Table 3's** error values. The models are tailored to each subject, due to the training set belonging exclusively to one of the subjects; therefore, they are less accurate when predicting the other subject's SBP and DBP.

A bigger set of high-quality ECG, PPG, and ABP signals, along with a higher number of unique subjects, would improve the models' ability to generalize to an independent dataset. More complex models, better suited to describe the non-linear relations that some of these features have with blood pressure, would characterize their relations better, as opposed to the simpler linear regression models used in this study, resulting in higher estimate accuracies.

6. FINAL REMARKS

Our MATLAB implementation enabled us to successfully extract a total of 21 blood pressure related features of the PPG's shape and time shift in relation to ECG as well as the values of SBP and DBP based on the ABP waveform.

From the PCA we could see that the main source of variance within our dataset stemmed from the source of the samples, meaning from which subject they were from. There was no clear predominance of variance explained by any of the features, therefore no dimensionality reduction was made based on that.

The estimation models created were based on a stepwise multivariate linear regression, enabling us to discard some of the features based on their statistical significance in the regression.

We found that, as expected, estimation models trained with data from a single subject presented an overestimation of their quality when testing with samples from the same subject.

Our cross-validation results revealed better MAE and STD values than the ones in the literature, mainly because our dataset dimensions are much more limited, thereby producing results with smaller MAE and STD, however, too overfitted for our specific pair of subjects.

The limited amount of interpretable data we were provided with, puts at stake the generalization of our models to feature data from other subjects, but on the other hand we are confident that our preprocessing and feature extraction pipeline can be employed to every dataset.

We can foresee an increase in accuracy of our model if other physiological features like the age, height and weight are included in the model, as blood pressure can be affected by these.

7. REFERENCES

[1] World Health Organization, "Global Brief on Hypertension: Silent Killer, Global Public Health Crisis," *World Heal. Organ.*, vol. 24, no. 1, pp. 2–2, 2014, doi: 10.5005/ijopmr-24-1-2.

[2] M. Nichols, N. Townsend, P. Scarborough, and M. Rayner, "Cardiovascular disease in Europe: Epidemiological update," *Eur. Heart J.*, vol. 34, no. 39, pp. 3028–3034, 2013, doi: 10.1093/eurheartj/eht356.

[3] S. L. Stevens *et al.*, "Blood pressure variability and cardiovascular disease: Systematic review and meta-analysis," *BMJ*, vol. 354, pp. 14–16, 2016, doi: 10.1136/bmj.i4098.

[4] N. Bruining, E. Caiani, C. Chronaki, P. Guzik, and E. Van Der Velde, "Acquisition and analysis of cardiovascular signals on smartphones: Potential, pitfalls and perspectives: By the Task Force of the e-Cardiology Working Group of European Society of Cardiology," *Eur. J. Prev. Cardiol.*, vol. 21, pp. 4–13, 2014, doi: 10.1177/2047487314552604.

[5] J. Sol, R. Delgado-gonzalo, and P. Guide, *The Handbook of Cuffless Blood Pressure Monitoring*. 2019.

[6] X. Ding, B. P. Yan, Y. Zhang, J. Liu, N. Zhao, and H. K. Tsang, "Pulse Transit Time Based Continuous Cuffless Blood Pressure Estimation : A New Extension and A Comprehensive Evaluation," *Sci. Rep.*, no. August, pp. 1–11, 2017, doi: 10.1038/s41598-017-11507-3.

[7] X. Xing, Z. Ma, M. Zhang, Y. Zhou, W. Dong, and M. Song, "An Unobtrusive and Calibration-free Blood Pressure Estimation Method using Photoplethysmography and Biometrics," *Sci. Rep.*, no. January, pp. 1–8, 2019, doi: 10.1038/s41598-019-45175-2.

[8] F. Miao *et al.*, "A Novel Continuous Blood Pressure Estimation Approach Based on Data Mining Techniques," vol. 2194, no. c, 2017, doi: 10.1109/JBHI.2017.2691715.

[9] M. Kachuee, S. Member, M. M. Kiani, and S. Member, "Cuff-Less Blood Pressure Estimation Algorithms for Continuous Health-Care Monitoring," vol. 9294, no. c, pp. 1–11, 2016, doi: 10.1109/TBME.2016.2580904.

[10] L. Wang, W. Zhou, Y. Xing, and X. Zhou, "Research Article A Novel Neural Network Model for Blood Pressure Estimation Using Photoplethesmography without Electrocardiogram," vol. 2018, 2018.

[11] "Multiparameter Intelligent Monitoring in Intensive Care II (MIMICII): A public-access intensive care unit database." https://physionet.org/content/mimiciii/1.4/.

[12] K. Takazawa *et al.*, "Assessment of vasoactive agents and vascular aging by the second derivative of photoplethysmogram waveform," *Hypertension*, vol. 32, no. 2, pp. 365–370, 1998, doi: 10.1161/01.HYP.32.2.365.

[13] D. J. Hughes, C. F. Babbs, L. A. Geddes, and J. D. Bourland, "Measurements of Young's Modulus of Elasticity of the Canine Aorta with Ultrasound," *Ultrason. Imaging*, vol. 1, no. 4, pp. 356–367, 1979, doi: 10.1177/016173467900100406.

[14] C. C. Y. Poon and Y. T. Zhang, "Cuff-less and noninvasive measurements of arterial blood pressure by pulse transit time," *Annu. Int. Conf. IEEE Eng. Med. Biol. - Proc.*, vol. 7 VOLS, pp. 5877–5880, 2005, doi: 10.1109/iembs.2005.1615827.

[15] Y. L. Zheng, B. P. Yan, Y. T. Zhang, and C. C. Y. Poon, "An armband wearable device for overnight and cuff-less blood pressure measurement," *IEEE Trans. Biomed. Eng.*, vol. 61, no. 7, pp. 2179–2186, 2014, doi: 10.1109/TBME.2014.2318779.

[16] R. A. Payne, C. N. Symeonides, D. J. Webb, and S. R. J. Maxwell, "Pulse transit time measured from the ECG: An unreliable marker of beat-to-beat blood pressure," *J. Appl. Physiol.*, vol. 100, no. 1, pp. 136–141, 2006, doi: 10.1152/japplphysiol.00657.2005.

[17] R. A. Chaudhry R, Miao JH, "Physiology, Cardiovascular.," *StatPearls [Internet]. Treasure Island (FL): StatPearls Publishing*. https://www.ncbi.nlm.nih.gov/books/NBK493197/.

[18] "stepwisefit." https://www.mathworks.com/help/stats/stepwisefit.html.

Authors' Bio:

Diogo Antunes

Email: diogoduarteantunes@tecnico.ulisboa.pt

4th year MSc Biomedical Engineering student at Instituto Superior Técnico. Main interests include: Neuroimaging, Signal Processing, Biophysics and Machine Learning.

Diogo Batista

Email: diogo.batista@tecnico.ulisboa.pt

4th year MSc Biomedical Engineering student at Instituto Superior Técnico. Interested in the medicine–engineering interface, specifically medical imaging, electronic gadgets, and signal processing.

Pedro Louro Costa Osório

Email: pedro.c.osorio@tecnico.ulisboa.pt

4th year MSc Biomedical Engineering student at Instituto Superior Técnico. Interested in medical imaging, bio signal acquisition and processing especially when applied to BCI.